ACS OMEGA

Open Access

http://pubs.acs.org/journal/acsodf

Article

Design and Synthesis of Red-Absorbing Fluoran Leuco Dyes Supported by Computational Screening

Vitor Angelo Fonseca Deichmann,* Dennis Chercka, David Danner, Silvia Rosselli, Gabriele Nelles, Anthony Roberts, and Vadim Rodin*

Cite This: *ACS Omega* 2024, 9, 34567−34576

Read Online

ACCESS | Metrics & More | Article Recommendations | Supporting Information

ABSTRACT: We report here on the design and synthesis of red-absorbing fluoran leuco dyes (LD). An essential part of the present dye development process is a computational screening of the candidate molecules, which allows for both time-efficient and accurate in silico characterization of the dyes. We focus our study here on the robust benzo[a]fluoran scaffold frequently used in leuco dyes. For the computational screening of LD candidates, an automated DFT-based simulation protocol has been developed and applied. The protocol consists of a combinatorial generation of the molecular structures of possible LD candidates, followed by simulations of their optimized molecular geometries, with their UV−Vis spectra as the main figure of merit. In the present application of the simulation protocol, more than 1600 structures of possible LD candidates have been evaluated. Finally, two structures, LD01 and LD02, have been chosen from the list of the best computed LD candidates to be synthesized and characterized. Our study demonstrates how the synergy between experiment and simulation can facilitate the design of novel leuco dyes.

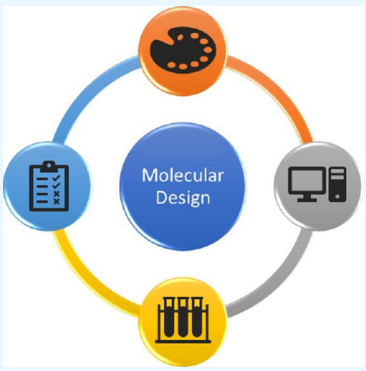

INTRODUCTION

Leuco dyes (LD) are materials that undergo controlled color changes resulting in a shift from a colorless (leuco) state to an intense color state that absorbs in the visible (λ = 380−700 nm), or even in the near−infrared region (λ = 700−1200 nm), depending on the molecular structure of the dye.[1−4] The change from the colorless to the colored state can be triggered by an acidic environment, which causes modifications of the molecular structure of the dye, i.e., by opening the lactone ring. Thereby a quinoidal system is formed, extending the conjugation length within the molecule, resulting in absorption at longer wavelengths, and thus, the dye appears colored. Figure 1 shows both the open (colored) and closed (colorless) forms in the switching process and photographs of a commercial dye dissolved in methyl ethyl ketone (MEK) with and without the addition of an acid. This process is reversible; upon proton subtraction, the lactone ring closes, and the molecule becomes transparent again.

For most commercial applications, the key features of leuco dyes are the absorption spectra of colored and colorless structures. Therefore, the design and synthesis of a new LD must be tailored for each desired color, with the color determined by its molecular structure. There are several classes of leuco dyes, with spiro[isobenzofuran- 1,9-xanthen]-3-one (also known as fluoran dyes) being one of the most popular, due to the versatility of their molecular structure modifications as well as the variety of applications, e.g. in thermo-printing,[5−7] textile,[8−11] biological applications,[12−14] etc.

A typical dye development protocol consists of several major steps, which are schematically depicted in Figure 2. The very first step is the molecular design, i.e., the creation of the molecular structures of the possible candidates. Considering the possible variations of substituents in the molecular structure, it is trivial to generate a list of candidates containing thousands of molecules. However, because it is not trivial to synthesize and characterize all these candidates, due to chemical, environmental, economic, and, of course, time constraints, computational screening can be used for in silico characterization of the candidate molecules. Such a screening can expedite the whole development process, resulting in marked improvements in terms of the development time and LD materials themselves, as the choice of promising candidates becomes more evident. In the next step of the development process, the computational results are analyzed and compared with the desired, targeted, specifications. The most suitable candidates are thus selected for synthesis and further detailed experimental analysis. Finally, if one or several of the selected candidates fulfill the specifications, the development process is deemed completed.

Received: March 18, 2024
Revised: June 20, 2024
Accepted: July 9, 2024
Published: August 2, 2024

https://doi.org/10.1021/acsomega.4c02646
ACS Omega 2024, 9, 34567−34576

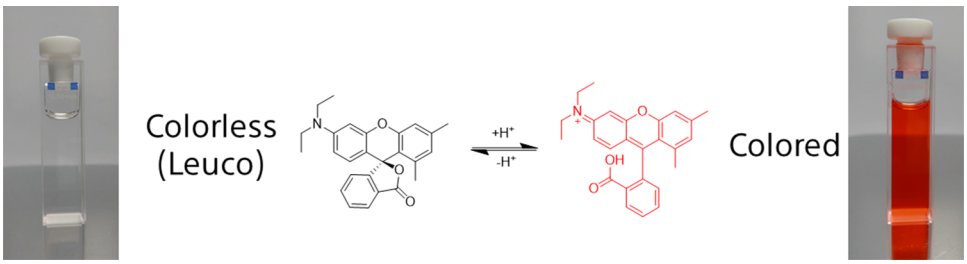

Figure 1. Leuco dye CD05(TCI) color switching.

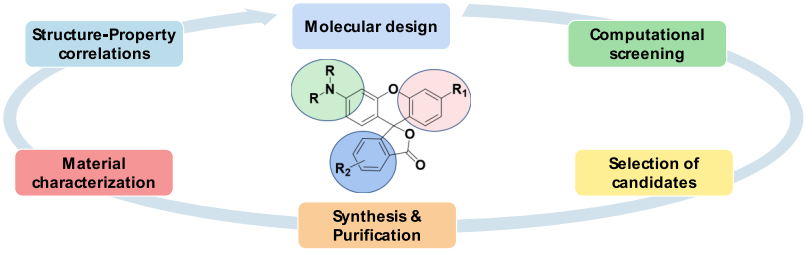

Figure 2. Iterative leuco dye design and development workflow.

Over recent decades, there are a plethora of examples of how computational screening methods have had a significant impact on how modern chemistry is conducted; such computational screening approaches were initially developed in pharmaceutical chemistry[15,16] and have expanded nowadays to fields as diverse as rapid COVID-19 antiviral drug discovery,[17−20] semiconductor development of organic[21−25]/ perovskite[26] solar cells, metal−organic framework discovery for gas storage/filtration,[27−29] or lithium ion batteries,[30] to name but a few examples in the field of (organic) materials chemistry.[31−35]

At the initial stage of our project to design and synthesize new LDs, it was already obvious that accurate computational methods of quantum chemistry (QC) would play an essential role in accelerating the dye design and development process. While a wealth of empirical knowledge on the tailoring of the LD absorption properties has been accumulated, it was expected that fast and efficient QC simulations could provide valuable information when selecting the synthesis targets. To this end, the position of the LD absorption maximum has been selected as a key dye property for computational screening.

However, as the QC simulations have limitations in their accuracy, one may run into the risk of missing or excluding viable candidates. Thus, it becomes indispensable to validate and calibrate the simulation methods by comparing the available experimental data to the simulation results. If necessary, the molecular design rules can also be readjusted accordingly. Thus, this development is purposefully an iterative, circular, process−as shown in Figure 2.

For a QC simulation engine in the computational screening, the Turbomole Program Package for electronic structure calculations was chosen.[36] The simulation protocol was developed iteratively to balance the predictive power of the simulations against the computational cost. The electronic structure calculations were performed at the density functional theory (DFT) and time-dependent DFT (TD-DFT) levels of theory as implemented in Turbomole version 7.6.[36,37]

As a first step, an initial version of the simulation protocol for the calculation of the absorption spectra of LDs was developed and validated by using commercial materials. After that, a two-step automated design and screening protocol was developed and applied for the simulation of hundreds of molecular structures that, to the best of our knowledge, are neither commercially available nor found in the literature. The target is to predict the desired features that will then support and facilitate the selection of a few, very targeted, candidates for synthesis (see the Results and Discussions part).

As such, finally, two structures, LD01 and LD02, were chosen from the list of the best computed candidates to be synthesized and characterized (see the Results and Discussions part). Initially, dye **LD01** was prepared due to it having the most promising properties predicted by the simulations, whereas **LD02** was selected due to its design containing additional withdrawing and donating groups. It was found by this simulation that the bis(trifluoromethyl)phenyl moiety does not adversely affect the absorption properties. Furthermore, from our prior experience, this moiety is expected to significantly improve the solubility.

EXPERIMENTAL SECTION

Chemicals and Methods. Unless otherwise specified, reagents were purchased from TCI, Sigma-Aldrich, and 2022 VWR International, LLC and used without further purification. Intermediate 12 was purchased from ChiroBlock GmbH and used as received. Solvents were of high purity grade as well as anhydrous in some cases and were used as obtained. All reactions were carried out under a nitrogen atmosphere. Column chromatography was carried out over either silica gel Merck-60, or irregular silica from VWR (60−200 μm). Thin layer chromatography (TLC) was performed on aluminum or plastic sheets precoated with silica gel 60 F254. ^{1}H NMR and ^{13}C NMR spectra were recorded on a Bruker AMX 400 MHz spectrometer. UV−Vis spectra were recorded on a Varian Cary spectrophotometer. Electron ionization mass spectra were obtained using the Agilent GC-MS system. Atmospheric solids analysis probe measurements with atmospheric pressure chemical ionization were performed on an Advion system Expression^{S} CMS.

Computational Details. The structure libraries for dye screening were built by using a combinatorial approach. Our

https://doi.org/10.1021/acsomega.4c02646
ACS Omega 2024, 9, 34567−34576

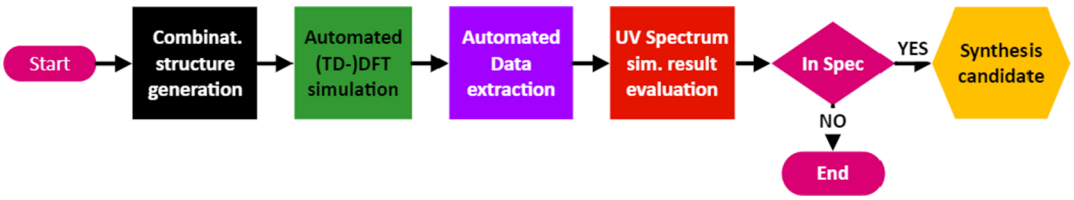

Figure 3. General Simulation Workflow of this Work.

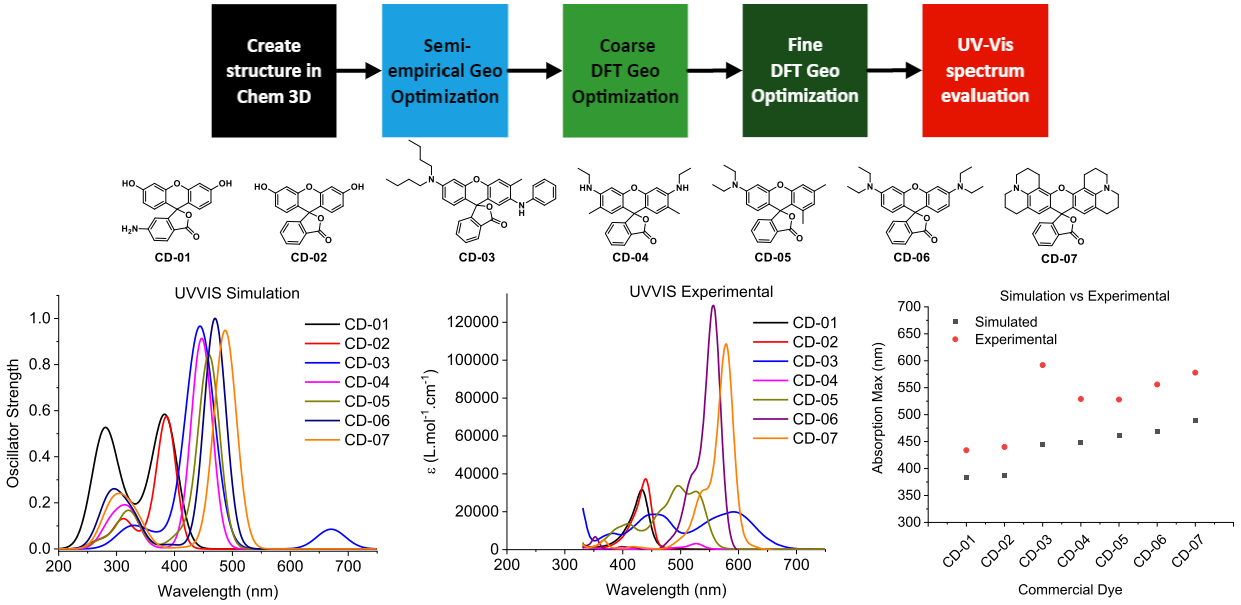

Figure 4. Simulation protocol scheme (top), molecular structures of simulated commercial leuco dyes (middle), and simulated spectra (bottom left) compared to experimental data (bottom right).

simulation workflow is shown in Figure 3. For initial combinatorial structure generation, the freeware package *Datawarrior* due to its high operational speed and *easy-to-use interface*. The database entries was exported as 3D models. The libraries of the structures were then prepared for DFT-based simulations by converting them into a compatible file format using *Openbabel*. The quantum chemical simulation suite in this work is Turbomole providing swift and high-quality (TD)-DFT simulations (see below for details). Simulated UV−Vis results were analyzed with an automated script, selecting candidates according to the wavelength of the highest oscillator strength transition. A detailed presentation of the workflow can be found in Figure S1.

RESULTS AND DISCUSSION

Simulation Protocol. As the first step, an unautomated version of the simulation protocol for the simulation of LD structures by using the Turbomole Molecular Simulation suite was developed and validated for commercial materials. A so-called "simulation template" was created in TmoleX (the GUI for Turbomole) to perform reliable and reproducible simulations of LD molecules. The key simulation output is the UV−VIS absorption spectrum (simulated by TD-DFT using a hybrid B3-LYP functional and the def2-TZVP basis set); furthermore, information on the frontier orbital energies and dipole moments was also obtained as significant outputs. An implicit solvent model (COSMO) was included in the TD-DFT UV−Vis spectrum simulation, to better predict the ex-silico leuco dye UV−Vis spectra. As model compounds, we used seven commercial LDs. The steps for the simulation are depicted below in Figure 4 (upper part) along with the molecular structures of the commercial dyes (middle part). In this case, the generation of structures was done manually using Chemdraw 20.0 (2D and 3D), and the simulation spectra were compared with experimental data obtained in methyl ethyl ketone solutions (10^{-5} M) in the presence of 1.0% trifluoracetic acid (v:v). The absorption spectra of molar extinction coefficient (ε) against wavelength were determined by a spectrophotometer, and ε was determined by $\epsilon = A/cl$, where A is absorbance (obtained by UV−Vis scan 320−750 nm), c is concentration, and l is the cuvette path length (equals 1.0 cm). From comparisons of the simulated and experimental absorption maxima, we observed a regular, consistent blue shift of the simulated maxima by about 50−80 nm. The comparison is presented in Figure 4, bottom part.

Therefore, for the usage of the current DFT simulation results with the current input parameters for reliable predictions, one can assume that the corresponding experimental results will be around 50−80 nm red-shifted for this class of materials. The consistency of this outcome is a very important consideration, because it supports the selection of new and unknown candidates, avoiding unnecessary synthesis, especially when there is no experimental evidence for comparison.

A further important comment is given regarding the results obtained for dye **CD-03**. This dye presents two absorption peaks, the first with the maximum around 430 nm and the second at 670 nm in the simulation, whereas in solution, the

https://doi.org/10.1021/acsomega.4c02646
ACS Omega 2024, 9, 34567−34576

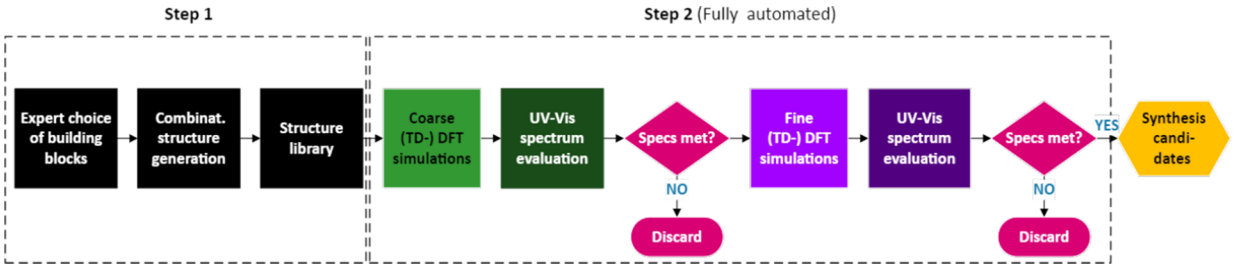

Figure 5. Main automated simulation workflow; see the text for more detail of the basic blocks.

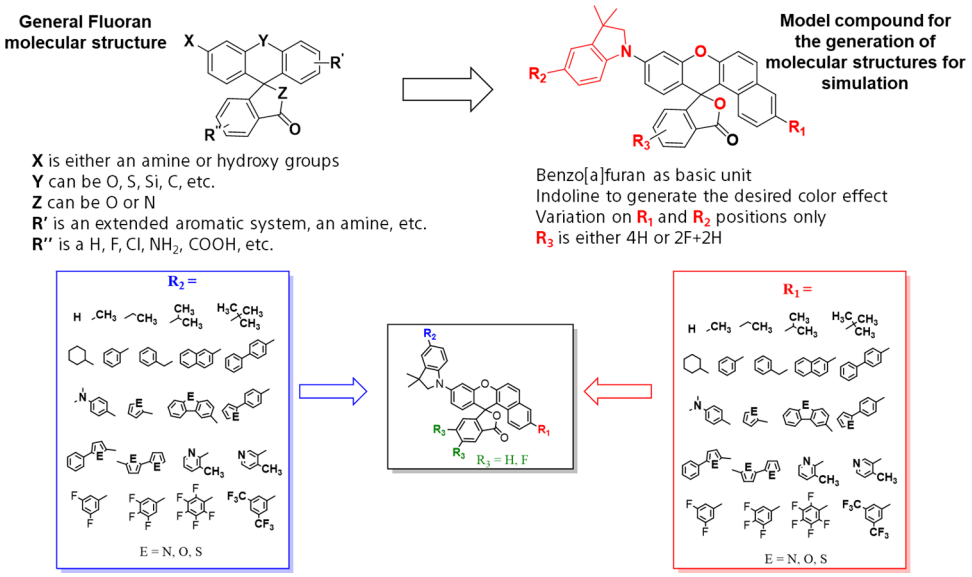

Figure 6. Creation of the structure library for red-absorbing leuco dyes.

two peaks are located at 450 and 590 nm, respectively, with a broad absorption band covering essentially the entire visible spectrum. Thus, by applying the aforementioned empirical correction of 50−80 nm, it is possible to obtain rather reliable predictions from the simulated absorption spectra, and hence, the simulation protocols can support the design of new molecules. However, the direct comparison between simulated and experimental results and finally the decision of which structure should be synthesized must be done carefully and with caution. It is important to note that there are more aspects that could be addressed while comparing simulation and experimental results, such as the usage of different solvents for a more detailed study of the optical properties or preparing solid state samples to evaluate aggregation effects, electrochemical analysis, as well as the study of thermal and electronic properties, but these aspects are out of the scope of this paper.

In addition, we stress that in the present work, we concentrate on the comparison of the simulated and observed absorption maxima as the primary figure of merit. To compare the calculated and experimental oscillator strengths, an additional analysis would be needed, and this is out of the scope of the present study.

The next development step was to automate the computational screening process. This simulation protocol for systematic and efficient screening of leuco dyes consists of two main steps, as shown in Figure 5. First, combinatorial generation of LD molecular structures was performed. If this was done fully automatically, allowing the whole gamut of possible combinations, then the list of possible candidates could become intractably long, containing at least many thousands of entries. Therefore, the initial choice of the molecular building blocks was constrained from the very beginning by our internal expert evaluation, that finally resulted in a set of slightly more than 1600 structures where we expected to have the greatest promise of success. After a library of molecular structures was prepared, we proceeded with the QC calculations for all the selected LD candidate molecules.

The computational screening itself is done in two steps: first the coarse screening and, if this is passed, then the second fine screening. Each step consists of DFT geometry optimization followed by TD-DFT calculation of the UV−Vis spectra for the optimized structure. This workflow is based on the validated, manual procedure outlined in Figure 4. The (TD)-DFT simulations are automated by bash scripting as well as the subsequent data extraction of the most relevant simulation results (HOMO/LUMO energies, the position of the main absorption peak, etc.). Only vertical UV−Vis transitions were considered, as this was deemed sufficient for the synthesis candidate selection, and additionally, the simulations including electron-vibronic coupling have a much higher computational cost. Finally, the simulation results were collated and provided to the user in the form of a Microsoft Excel table. This procedure allows for fast evaluation of the key simulation results, even for users with limited experience in computational chemistry.

Results of the Computational Screening. The selection of the model compound and the definition of the structural variations is a key step because it determines where the dye will

https://doi.org/10.1021/acsomega.4c02646
ACS Omega 2024, 9, 34567−34576

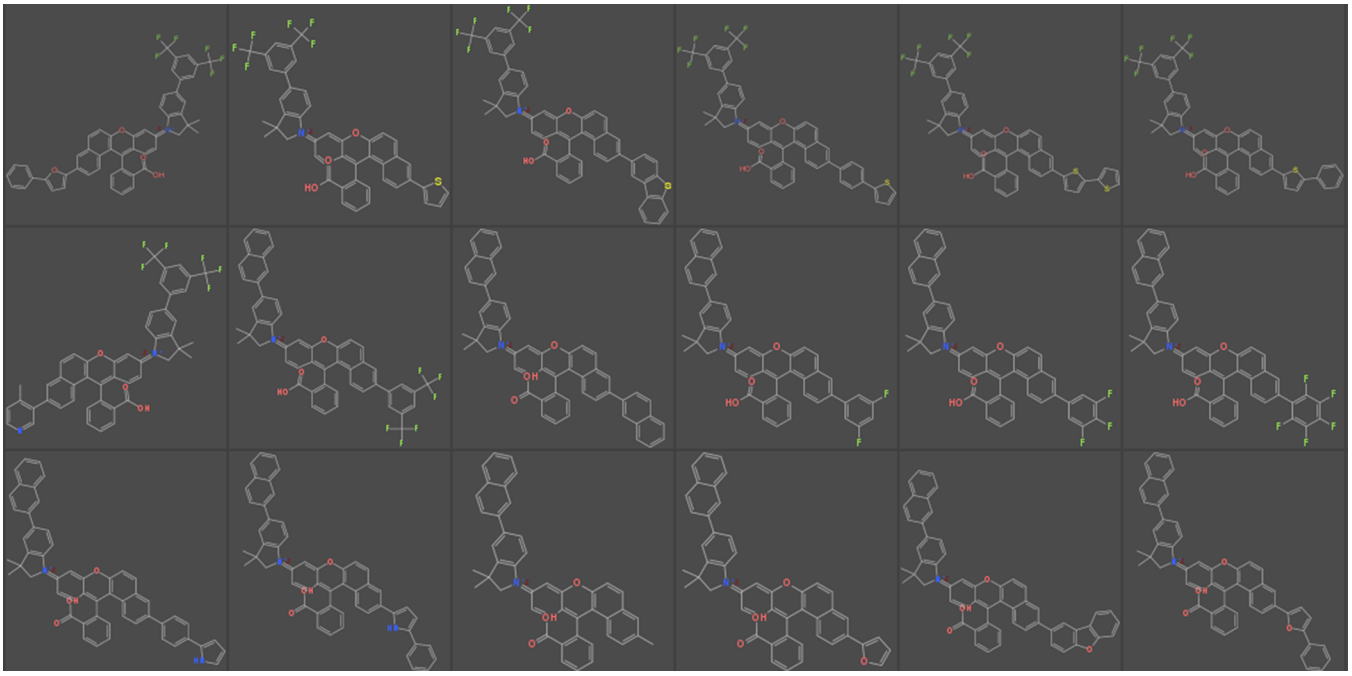

Figure 7. Screenshot from some of the sample structure sequences resulting from the combinatorial structure generation.

absorb.[1] Considering the general structure of fluoran dyes (see Figure 6), as well as keeping open the possibility of any structural modification, one can easily generate thousands of substructures.

Moreover, as our objective here is not to screen as many structures as possible but instead to develop a simulation tool that reliably predicts absorption spectra of unknown, but still relevant, structures, we therefore decided to specify some parts of the structure and to generate a reasonable, tractable number of molecules based on this model. As such, we decided to focus on unknown structures to create a method to predict absorption spectra of dyes. Therefore, we chose an indoline structure containing benzo[a]fluorans that, to the best of our knowledge, have not been reported yet. It is important to note that the structure could have been benzo[b]fluoran or a different amine instead, yet the crucial point for us was to create new or unknown structures. Moreover, we know that the indoline moiety promotes a redshift in the absorption spectra,[38] and our expectation, prior to simulations, is that any such structure would have absorption in the red, or even in the near-infrared region.

Keeping this in mind, we established our target to obtain experimental absorption maxima in the range between 550 and 650 nm, with the expectation that the absorption band could reach 700 nm. Practical considerations mean that although simulation tools give us freedom to simulate thousands of molecules, from the synthesis point of view, we should keep the structure feasible; that is, for the design of a new molecule, one should keep in mind the availability of reagents, solvents, etc., as well as their cost, toxicity, and last, but not the least, to combine the information found in procedures and protocols for synthesis available in the literature, in other words, to be sure that the molecule can be synthesized. By taking into consideration the above arguments, a library with ca. 1600 structures, containing electron donating and withdrawing groups (see Figure 6), has been created, and the corresponding absorption spectra have been simulated.

For the molecular structure generation, the combinatorial chemistry tools *Chemfinder* (component of PerkinElmer *ChemOffice20* Suite[39]) and the freeware package *Datawarrior*[40] were used. From our experience, *Datawarrior* was better suited for the combinatorial generation of fluoran-type leuco dyes. Furthermore, the software performance when generating large combinatorial libraries was superior to that of *Chemfinder* (we found that libraries containing around 1 M structures can be created by Datawarrior within 30 min on a standard laptop). Three-dimensional not-optimized structures corresponding to the colored states of the leuco dyes of interest were straightforwardly generated by the software in XYZ format (Figure 7).

It is important to bear in mind that the size of a structure library will depend on only the number of building blocks that are used. However, some of those blocks may cause only miniscule changes in the electronic structure (sometimes far from the desired color) with only slight changes in the absorption spectra. On the other hand, e.g., the solubility and therefore later processability may be significantly affected by this modification. Furthermore, in this work, we decided to skip the use of, for instance, alkoxy, amine, or sulfur-based building blocks directly attached to the xanthene moiety of the fluoran dyes, since they would bring more complexity to the list, resulting in a strong cost for the simulation time, as well as an undesired and expected red-shift of the absorption spectra due to electron-donating effect. This proves that the modifications to the molecular structure proposed in the structure library may change the color of the dyes, but with a proper selection criterion, we can select the structures that are more suitable to the project's targets and needs.

In the simulation protocol, the molecular structure of each LD candidate is optimized in three steps, starting from the structures generated by *Datawarrior*. An initial preoptimization is performed semiempirically (AM1), followed by two-step optimization at the density functional theory level of theory. In the first, coarse, DFT geometry optimization the PBE GGA

https://doi.org/10.1021/acsomega.4c02646
ACS Omega 2024, 9, 34567−34576

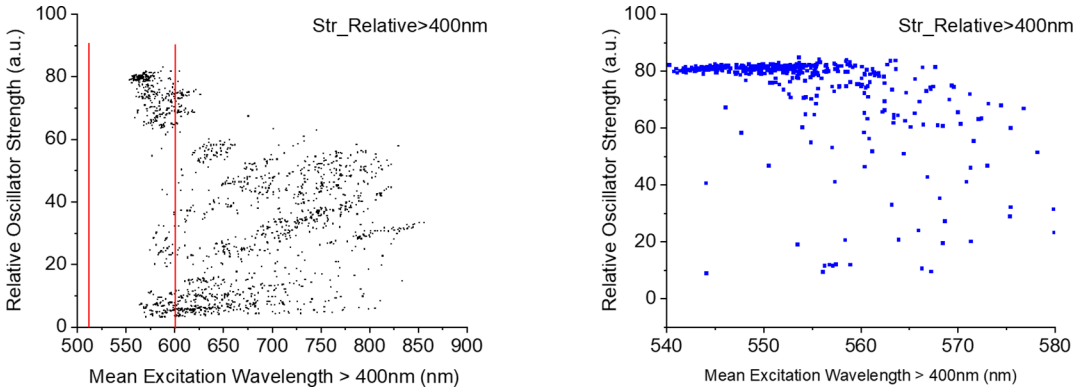

Figure 8. Left: Results of first screening iteration. 531 structures meet the selection criterion. Right: Results of second screening iteration show that ca. 400 structures meet the restrictive selection criterion.

functional and the def2-SV(P) basis set are used.[41] The optimization is followed by the simulation of the UV−Vis absorption spectra on a TD-DFT level with the same choice of the functional and the basis set (usually 5 transitions are calculated). For the transitions with $\lambda \geq 400$ nm in the visible region, a weighted average wavelength is calculated according to $\bar{\lambda} = \sum_i \lambda_i f_i / \sum_i f_i$, where λ_i is the calculated excitation wavelength and f_i is the corresponding oscillator strength.

After the first coarse screening step, we observed a large number of structures with simulated absorption maxima above 700 nm (some even beyond 800 nm). This means that the maximum corrected for the simulation offset would lie in the near-infrared region after the aforementioned considerations and comparisons with the results obtained for the commercial dyes presented in Figure 4. Thus, we decided to restrict the list of the relevant structures for a second high fidelity simulation run by limiting the potential candidates to those that absorb within the visible range.

In the second, high fidelity, simulation run, fine geometry optimization is performed using a hybrid B3-LYP functional and the def2-TZVP basis set, with the COSMO solvent model activated (the dielectric constant is set to $\varepsilon = 18$ to emulate the solvent methyl ethyl ketone).[42] The UV−Vis absorption properties are simulated on a TD-DFT level (B3-LYP/def2-TZVP/COSMO). During this simulation run, we observed that, as expected, as the accuracy of the simulations increased, so did the computational cost; therefore, we decided to restrict the range of absorption even further, and therefore only the structures with the mean absorption wavelength 540 nm < $\bar{\lambda}$ < 580 nm from the first screening step were considered as suitable candidates (see Figure 8). As mentioned at the beginning of this section, the extraction of the main simulation results from the `stdout` Turbomole files and their collation in a tabular form was automated by bash scripting. The final automatically generated tabulated text file was imported into an Excel overview table to facilitate the rapid selection of appropriate LD candidates, even for users with limited experience in computational chemistry.

As discussed in the previous subsection, the simulation protocol was validated by comparison of the simulated UV−Vis spectra with experimental spectra for eight commercial LDs; because a systematic blueshift of $\Delta\lambda \approx 50-80$ nm of the calculated absorption maxima versus experiment was observed, a broader specification region was defined, in order not to exclude potentially valuable candidates. In the result, ca. 400 structures from the original database meet the selection criterion of 540 nm < $\bar{\lambda}$ < 580 nm (see Figure 8). Then, the simulation protocol described in the previous subsection was applied, and the UV−Vis spectra were calculated and analyzed. Currently, no clear structure−property correlation leading to the offset can be identified.

Further narrowing the targeted predicted mean absorption wavelength interval to, for instance, 540 nm < $\bar{\lambda}$ < 560 nm, still yields slightly above 300 hits (keeping in mind that the number of known red-absorbing benzo[a]fluoran leuco dyes is limited); this large number of suitable candidates illustrates that the initial selection of building blocks (Figure 6) for this screening was well justified.

It is noteworthy that the automated QC simulation protocol devised in the present work can be easily modified to screen for some different molecular properties, e.g., IP, EA, or similar, and also for other families of organic molecules different from leuco dyes. The actual bottleneck for the computational screening of the current work is the combinatorial choice of all possible candidates, as it leads to such a huge list of molecules that makes the computational screening of all of them intractable given the currently available simulation capabilities. This is why expert intervention was needed in this work in order to limit the initial huge plurality of candidates to a tractable number. Maybe, in the future, some ML approaches will assist in overcoming this current restriction.

Synthesis and Structure Determination of the Selected Leuco Dyes. The choice of the relevant substituents in this work was guided by "chemical intuition", and for the decision whether to attempt the test-scale preparation, the candidates were assessed further for synthetic complexity and number of steps, solubility, reactivity, cost, availability of building blocks, and literature results and intellectual property status. Internally, project-specific development needs were best met by **LD01** and **LD02**, and these two structures were selected for synthesis (Figure 9).

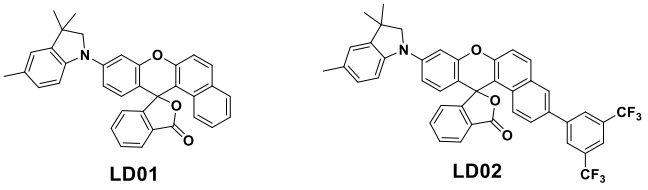

Figure 9. Molecular structures of LD01 and LD02.

https://doi.org/10.1021/acsomega.4c02646
ACS Omega 2024, 9, 34567−34576

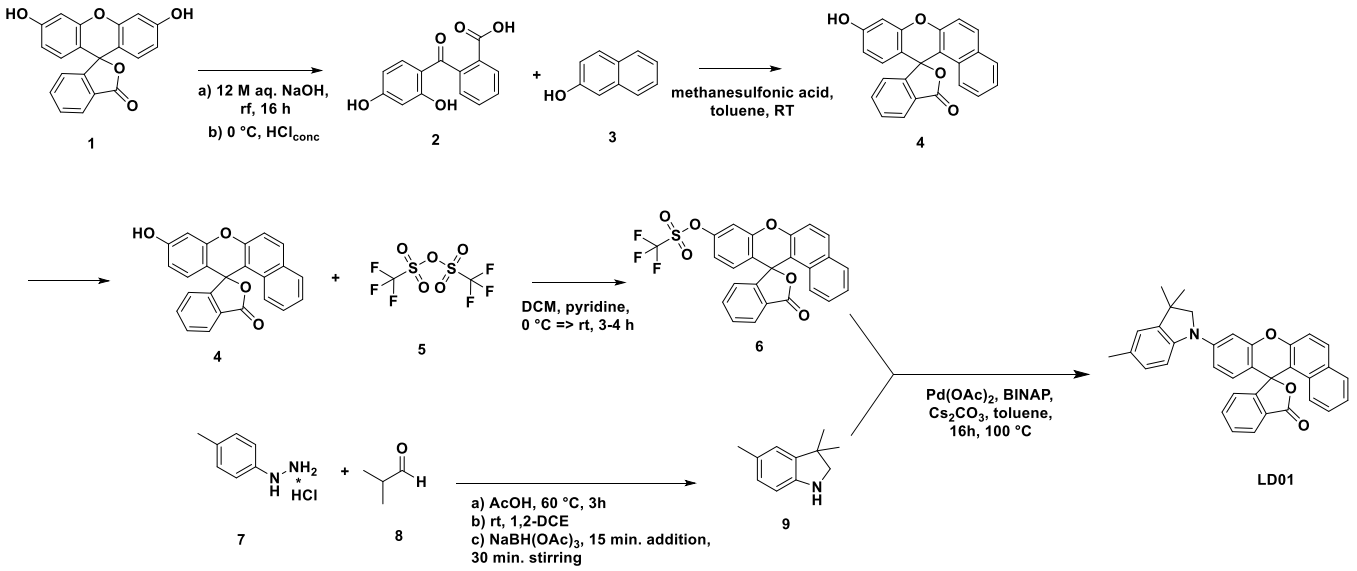

Figure 10. Synthesis of LD01.

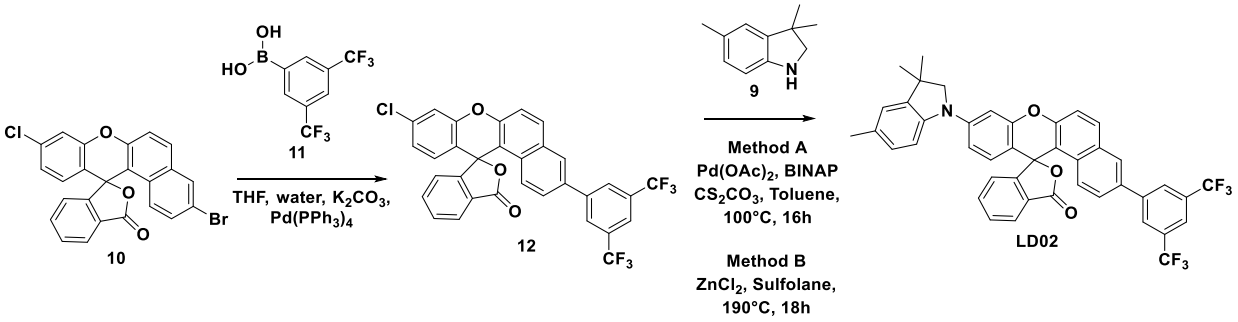

Figure 11. Synthesis of LD02.

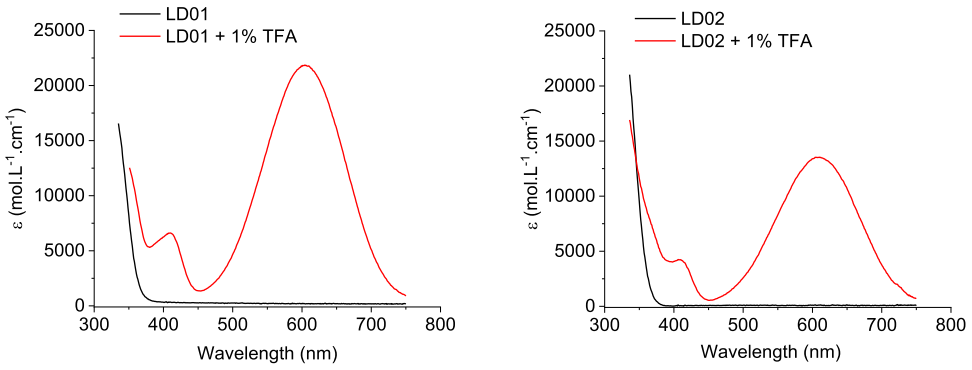

Figure 12. UV−Vis spectra of LD01 (left) and LD02 (right) recorded in MEK before (black curve) and after the addition of 1% TFA (red curve).

For the preparation of **LD01,** a four-step synthesis route was employed (Figure 10). First, dihydroxybenzoylbenzoic acid (**2**) was synthesized by the partial hydrolysis of fluorescein (**1**) under alkaline conditions. The building block was received in excellent yield and reacted with naphthol to provide benzo[a]fluoran (**4**) in a condensation step with reasonable yields. The remaining hydroxy function was converted to the corresponding triflate (**6**) in excellent yields. The required indoline donor unit (**9**) was prepared by reaction of the respective toluidine hydrazine hydrochloride and aldehyde precursors.[43] Yield from the unoptimized reaction was rather low; however, the received amount of material was sufficient for the following reaction steps.

Buchwald−Hartwig-type cross-coupling reaction conditions were applied for reacting triflate (**6**) with indoline (**9**) providing target leuco dye **LD01** in moderate yields. The synthesis was completed after five steps.

For the synthesis of **LD02,** the route previously applied for **LD01** was revised (Figure 11). The bromo-chloro-benzo[a]fluoran (**10**) was chemo-selectively reacted with boronic acid (**11**) under Suzuki-type cross-coupling conditions using $Pd(PPh_3)_4$ as a catalyst. Intermediate (**12**) was obtained in good yields. For the final step, we tested the Buchwald−Hartwig-type cross-coupling reaction with the same conditions used for LD01. However, the results were very disappointing, with conversion yields around 3% after purification.

https://doi.org/10.1021/acsomega.4c02646
ACS Omega 2024, 9, 34567−34576

Clearly, the catalytic system applied for this reaction with chloride did not work as it did for triflates. From literature search, we found that different catalysts could be applied, but we decided to test a procedure that uses zinc chloride (a Lewis-acid mediated reaction) under elevated temperatures, also for indolines, and by applying these conditions, **LD02** was obtained with better conversion yields.[44,45] We confirmed the presence of the target material in larger amounts with a reasonable purity. There were not many impurities or side products visible on TLC. An important note here is that, although simulation protocols optimize the selection of new candidates, the laboratory challenges remain and sometimes cannot be overcome, and as mentioned before, the decision on which route is most suitable always depends on the costs, time constraints, yield, etc.

Leuco Dye Optoelectronic Characterization. The UV−Vis absorption spectra of **LD01** (left panel) and **LD02** (right panel) are shown in Figure 12. The absorption spectra of **LD01** in leuco and colored form were recorded in 10^{-5} M solution in MEK. Due to company internal guidelines and MEK being a common organic solvent for technical processing, it was chosen for photophysical characterizations in this work. The absorption maximum of the leuco state is in the UV region, below λ = 350 nm. Upon addition of trifluoroacetic acid (TFA), the colored state is formed, and its absorption maximum is located at λ = 604 nm with an extinction coefficient of ca. $\varepsilon = 2.2 \times 10^4$ $M^1 \times cm^1$ and a fwhm = 131 nm.

Analogous to **LD01**, the absorption spectra of **LD02** in leuco and colored form were determined in a 10^{-5} M solution in MEK. The absorption maximum of the leuco state is in the UV region, below λ = 350 nm. Upon the addition of TFA, the colored state is formed. The absorption maximum of the colored state is located at λ = 608 nm with an extinction coefficient of $\varepsilon = 1.4 \times 10^4$ $M^{-1} \times cm^{-1}$ and a fwhm = 135 nm. Both dyes are virtually colorless in the leucostate; extinction coefficients exceeding the noise level are observed only below λ = 400 nm. In the colored state, intense absorption in the red region is observed. The absorption maxima are located at similar positions with comparable fwhm, and **LD01** shows about 50% higher extinction coefficient.

The comparison between simulation and experimental spectra is shown in Figure 13. A reasonable agreement between those is achieved using the screening protocol. For **LD01** (black) and **LD02** (red), TD-DFT simulations predict the absorption maximum of the colored state to be located at λ = 554 and λ = 558 nm ($\Delta\lambda$ = 4 nm), respectively. The oscillator strength is 1.47 au compared to 0.84 au (~43% intensity for **LD02** compared to **LD01**). The experimental results in MEK + 1% TFA show a redshift of the main absorption signal of about $\Delta\lambda \approx 50$ nm. Nevertheless, the predicted differences between the two dyes are also found in the experiment. The **LD02** absorption maximum is red-shifted by $\Delta\lambda$ = 4 nm, and its intensity is 36% lower.

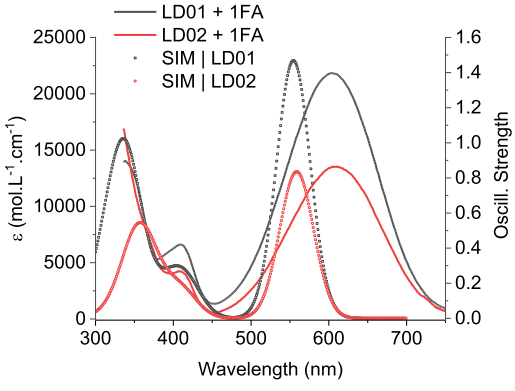

Figure 13. Solid lines: Experimental absorption spectra of LD-C01 (black) and LD-C02 (red) in MEK and 1% TFA. TD-DFT (B3-LYP, def2-TZVP) simulation results of the dyes in the colored state.

CONCLUSIONS

In this paper, we report on design and synthesis of red-absorbing fluoran leuco dyes. An essential part of the dye development process is a computational screening of the candidate molecules that allows time-efficient and at the same time accurate in silico characterization of the dyes.

We focus our study here on the robust benzo[a]fluoran scaffold frequently used in leuco dyes, with the indoline-containing benzo[a]fluoran, as it is expected that this moiety should promote a redshift in the absorption spectra.

For the computational screening of LD candidates, an automated QC simulation protocol was developed and applied. The protocol consists of a combinatorial generation of molecular structures of possible LD candidates, followed by two-step, coarse and fine, (TD-)DFT simulations of optimized molecular geometries and their UV−Vis spectra as the main figure of merit. In the present application of the simulation protocol, more than 1600 structures of possible LD candidates have been evaluated.

Finally, two structures, LD01 and LD02, were chosen from the list of the best computed LD candidates to be synthesized and characterized. Initially, the former dye was prepared as having promising properties predicted by the simulations, while LD02 was designed to contain additional withdrawing and donating groups.

Our study shows how the synergy between experiment and simulation can facilitate the design of novel leuco dyes.

ASSOCIATED CONTENT

Supporting Information

The Supporting Information is available free of charge at https://pubs.acs.org/doi/10.1021/acsomega.4c02646.

Details of synthesis of dyes and intermediates as well as their characterization data (PDF)

AUTHOR INFORMATION

Corresponding Authors

Vitor Angelo Fonseca Deichmann − *Sony Semiconductor Solutions Europe, Sony Europe B.V., 70327 Stuttgart, Germany*; orcid.org/0009-0005-1774-9274; Email: vitor.deichmann@sony.com

Vadim Rodin − *Sony Semiconductor Solutions Europe, Sony Europe B.V., 70327 Stuttgart, Germany*; Email: vadim.rodin@sony.com

Authors

Dennis Chercka − *Sony Semiconductor Solutions Europe, Sony Europe B.V., 70327 Stuttgart, Germany*

David Danner − *Sony Semiconductor Solutions Europe, Sony Europe B.V., 70327 Stuttgart, Germany*

Silvia Rosselli − *Sony Semiconductor Solutions Europe, Sony Europe B.V., 70327 Stuttgart, Germany*

https://doi.org/10.1021/acsomega.4c02646
ACS Omega 2024, 9, 34567−34576

Gabriele Nelles − *Sony Semiconductor Solutions Europe, Sony Europe B.V., 70327 Stuttgart, Germany*
Anthony Roberts − *Sony Semiconductor Solutions Europe, Sony Europe B.V., 70327 Stuttgart, Germany*

Complete contact information is available at: https://pubs.acs.org/10.1021/acsomega.4c02646

Author Contributions

The manuscript was written through contributions of all authors. All authors have given approval to the final version of the manuscript.

Notes

The authors declare no competing financial interest.

■ ACKNOWLEDGMENTS

The authors acknowledge the members of the Yuriko Kaino and Yuki Oishi teams, from Sony Semiconductor Solutions Corporation. We are thankful for their collaborative spirit, and support throughout the project.

■ ABBREVIATIONS

LD, leuco dyes; MEK, methyl ethyl ketone; QC, quantum chemistry; DFT, density functional theory; TD-DFT, time-dependent DFT; TLC, thin layer chromatography

■ REFERENCES

(1) Muthyala, R. *Chemistry and Applications of Leuco Dyes*; Springer: US, 2006.
(2) Shirasaki, Y.; Okamoto, Y.; Muranaka, A.; Kamino, S.; Sawada, D.; Hashizume, D.; Uchiyama, M. Fused-Fluoran Leuco Dyes with Large Color-Change Derived from Two-Step Equilibrium: iso-Aminobenzopyranoxanthenes. *Journal of Organic Chemistry* **2016**, *81* (23), 12046−12051.
(3) Meiqin, S.; yun, S.; Qiyu, T. Synthesis of fluoran dyes with improved properties. *Dyes Pigm.* **1995**, *29* (1), 45−55.
(4) Liu, D.; He, Z.; Zhao, Y.; Yang, Y.; Shi, W.; Li, X.; Ma, H. Xanthene-Based NIR-II Dyes for In Vivo Dynamic Imaging of Blood Circulation. *J. Am. Chem. Soc.* **2021**, *143* (41), 17136−17143.
(5) Kulčar, R.; Friškovec, M.; Hauptman, N.; Vesel, A.; Gunde, M. K. Colorimetric properties of reversible thermochromic printing inks. *Dyes Pigm.* **2010**, *86* (3), 271−277.
(6) Yanagita, M.; TakahashiI, S.; Aoki, I. Development of High Lightfast Fluoran Leuco Dyes for Thermosensitive Recording Papers. *J. Jpn. Soc. Colour Mater.* **1996**, *69* (10), 649−657.
(7) Eckardt, M.; Kubicova, M.; Tong, D.; Simat, T. J. Determination of color developers replacing bisphenol A in thermal paper receipts using diode array and Corona charged aerosol detection—A German market analysis 2018/2019. *Journal of Chromatography A* **2020**, *1609*, No. 460437.
(8) Zhang, W.; Fei, L.; Zhang, J.; Chen, K.; Yin, Y.; Wang, C. Durable and tunable temperature responsive silk fabricated with reactive thermochromic pigments. *Prog. Org. Coat.* **2020**, *147*, No. 105697.
(9) Oda, H. Photostabilization of organic thermochromic pigments. Part 2: Effect of hydroxyarylbenzotriazoles containing an amphoteric counter-ion moiety on the light fastness of color formers. *Dyes Pigm.* **2008**, *76* (2), 400−405.
(10) Oda, H. New developments in the stabilization of leuco dyes: effect of UV absorbers containing an amphoteric counter-ion moiety on the light fastness of color formers. *Dyes Pigm.* **2005**, *66* (2), 103−108.
(11) Du, Z.; Liu, J.; Gai, H.; Sheng, L.; Zhang, S. X.-A. A high-performance visible laser rewritable black paper. *Journal of Materials Chemistry C* **2020**, *8* (34), 11675−11680.
(12) Wang, L.; Du, W.; Hu, Z.; Uvdal, K.; Li, L.; Huang, W. Hybrid Rhodamine Fluorophores in the Visible/NIR Region for Biological Imaging. *Angew. Chem., Int. Ed.* **2019**, *58* (40), 14026−14043.
(13) Wang, L.; Barth, C. W.; Sibrian-Vazquez, M.; Escobedo, J. O.; Lowry, M.; Muschler, J.; Li, H.; Gibbs, S. L.; Strongin, R. M. Far-Red and Near-Infrared Seminaphthofluorophores for Targeted Pancreatic Cancer Imaging. *ACS Omega* **2017**, *2* (1), 154−163.
(14) Zhang, M.; Liu, X.; Yang, M.; Zheng, S.; Bai, Y.; Yang, B.-Q. A series of deep red fluorescent dyes: synthesis, theoretical calculations and bioimaging applications. *Tetrahedron Lett.* **2015**, *56* (41), 5681−5688.
(15) Chini, M. G.; Lauro, G.; Bifulco, G. Addressing the Target Identification and Accelerating the Repositioning of Anti-Inflammatory/Anti-Cancer Organic Compounds by Computational Approaches. *Eur. J. Org. Chem.* **2021**, *2021* (21), 2966−2981.
(16) Jenwitheesuk, E.; Horst, J. A.; Rivas, K. L.; Van Voorhis, W. C.; Samudrala, R. Novel paradigms for drug discovery: computational multitarget screening. *Trends Pharmacol. Sci.* **2008**, *29* (2), 62−71.
(17) Bocci, G.; Bradfute, S. B.; Ye, C.; Garcia, M. J.; Parvathareddy, J.; Reichard, W.; Surendranathan, S.; Bansal, S.; Bologa, C. G.; Perkins, D. J.; Jonsson, C. B.; Sklar, L. A.; Oprea, T. I. Virtual and In Vitro Antiviral Screening Revive Therapeutic Drugs for COVID-19. *ACS Pharmacology & Translational Science* **2020**, *3* (6), 1278−1292.
(18) Wang, J. Fast Identification of Possible Drug Treatment of Coronavirus Disease-19 (COVID-19) through Computational Drug Repurposing Study. *J. Chem. Inf. Model.* **2020**, *60* (6), 3277−3286.
(19) Wang, X.; Guan, Y. COVID-19 drug repurposing: A review of computational screening methods, clinical trials, and protein interaction assays. *Medicinal Research Reviews* **2021**, *41* (1), 5−28.
(20) Yu, R.; Chen, L.; Lan, R.; Shen, R.; Li, P. Computational screening of antagonists against the SARS-CoV-2 (COVID-19) coronavirus by molecular docking. *Int. J. Antimicrob. Agents* **2020**, *56* (2), No. 106012.
(21) Cui, Y.; Zhu, P.; Liao, X.; Chen, Y. Recent advances of computational chemistry in organic solar cell research. *Journal of Materials Chemistry C* **2020**, *8* (45), 15920−15939.
(22) Forero-Martinez, N. C.; Lin, K.-H.; Kremer, K.; Andrienko, D. Virtual Screening for Organic Solar Cells and Light Emitting Diodes. *Adv. Sci.* **2022**, *9* (19), No. 2200825.
(23) Greenstein, B. L.; Hutchison, G. R. Organic Photovoltaic Efficiency Predictor: Data-Driven Models for Non-Fullerene Acceptor Organic Solar Cells. *J. Phys. Chem. Lett.* **2022**, *13* (19), 4235−4243.
(24) Kanal, I. Y.; Owens, S. G.; Bechtel, J. S.; Hutchison, G. R. Efficient Computational Screening of Organic Polymer Photovoltaics. *J. Phys. Chem. Lett.* **2013**, *4* (10), 1613−1623.
(25) Rodríguez-Martínez, X.; Pascual-San-José, E.; Campoy-Quiles, M. Accelerating organic solar cell material's discovery: high-throughput screening and big data. *Energy Environ. Sci.* **2021**, *14* (6), 3301−3322.
(26) Emery, A. A.; Saal, J. E.; Kirklin, S.; Hegde, V. I.; Wolverton, C. High-Throughput Computational Screening of Perovskites for Thermochemical Water Splitting Applications. *Chem. Mater.* **2016**, *28* (16), 5621−5634.
(27) Altintas, C.; Altundal, O. F.; Keskin, S.; Yildirim, R. Machine Learning Meets with Metal Organic Frameworks for Gas Storage and Separation. *J. Chem. Inf. Model.* **2021**, *61* (5), 2131−2146.
(28) Tarzia, A.; Jelfs, K. E. Unlocking the computational design of metal−organic cages. *Chem. Commun.* **2022**, *58* (23), 3717−3730.
(29) Yan, Y.; Zhang, L.; Li, S.; Liang, H.; Qiao, Z. Adsorption behavior of metal-organic frameworks: From single simulation, high-throughput computational screening to machine learning. *Comput. Mater. Sci.* **2021**, *193*, No. 110383.
(30) Xiao, Y.; Miara, L. J.; Wang, Y.; Ceder, G. Computational Screening of Cathode Coatings for Solid-State Batteries. *Joule* **2019**, *3* (5), 1252−1275.
(31) Greenaway, R. L.; Jelfs, K. E. Integrating Computational and Experimental Workflows for Accelerated Organic Materials Discovery. *Adv. Mater.* **2021**, *33* (11), No. 2004831.

(32) Grynova, G.; Lin, K.-H.; Corminboeuf, C. Read between the Molecules: Computational Insights into Organic Semiconductors. *J. Am. Chem. Soc.* **2018**, *140* (48), 16370−16386.
(33) Jackson, K.; Jaffar, S. K.; Paton, R. S. Computational organic chemistry. *Annu. Rep. Prog. Chem., Sect. B: Org. Chem.* **2013**, *109*, 235−255. (0),
(34) Saeki, A.; Kranthiraja, K. A high throughput molecular screening for organic electronics via machine learning: present status and perspective. *Jpn. J. Appl. Phys.* **2020**, *59*, No. SD0801. (SD),
(35) Wang, L.; Nan, G.; Yang, X.; Peng, Q.; Li, Q.; Shuai, Z. Computational methods for design of organic materials with high charge mobility. *Chem. Soc. Rev.* **2010**, *39* (2), 423−434.
(36) TURBOMOLE V7.6 2021. *A development of University of Karlsruhe and Forschungszentrum Karlsruhe GmbH, 1989−2007*, 2007. TURBOMOLE GmbH since 2007; available from http://www.turbomole.com.
(37) Balasubramani, S. G.; Chen, G. P.; Coriani, S.; Diedenhofen, M.; Frank, M. S.; Franzke, Y. J.; Furche, F.; Grotjahn, R.; Harding, M. E.; Hättig, C.; Hellweg, A.; Helmich-Paris, B.; Holzer, C.; Huniar, U.; Kaupp, M.; Marefat Khah, A.; Karbalaei Khani, S.; Müller, T.; Mack, F.; Nguyen, B. D.; Parker, S. M.; Perlt, E.; Rappoport, D.; Reiter, K.; Roy, S.; Rückert, M.; Schmitz, G.; Sierka, M.; Tapavicza, E.; Tew, D. P.; van Wüllen, C.; Voora, V. K.; Weigend, F.; Wodyński, A.; Yu, J. M. TURBOMOLE: Modular program suite for ab initio quantum-chemical and condensed-matter simulations. *J. Chem. Phys.* **2020**, *152* (18), No. 184107.
(38) Grimm, J. B.; Lavis, L. D. Synthesis of Rhodamines from Fluoresceins Using Pd-Catalyzed C−N Cross-Coupling. *Org. Lett.* **2011**, *13* (24), 6354−6357.
(39) *PerkinElmer Informatics, ChemOffice20*.
(40) Sander, T.; Freyss, J.; von Korff, M.; Rufener, C. DataWarrior: An Open-Source Program For Chemistry Aware Data Visualization And Analysis. *J. Chem. Inf. Model.* **2015**, *55* (2), 460−473.
(41) Perdew, J. P.; Yue, W. Accurate and simple density functional for the electronic exchange energy: Generalized gradient approximation. *Phys. Rev. B* **1986**, *33* (12), 8800−8802.
(42) Becke, A. D. A new mixing of Hartree−Fock and local density-functional theories. *J. Chem. Phys.* **1993**, *98* (2), 1372−1377.
(43) Woolford, A. J.-A.; Howard, S.; Buck, I. M.; Chessari, G.; Johnson, C. N.; Tamanini, E.; Day, J. E. H.; Chiarparin, E.; Heightman, T. D.; Frederickson, M.; Griffiths-Jones, C. M. *Preparation of bicyclic heterocycles as anticancer agents*, 2012.
(44) Woodroofe, C. C.; Lim, M. H.; Bu, W.; Lippard, S. J. Synthesis of isomerically pure carboxylate- and sulfonate-substituted xanthene fluorophores. *Tetrahedron* **2005**, *61* (12), 3097−3105.
(45) Cheon, K.-S.; Filosa, M. P.; Marshall, J. L.; Hasan, F. B.; Skyler, D. A.; Telfer, S. J.; Hardin, J. M. Novel dyes and use thereof in imaging members and methods. WO2009097433, 2009.

https://doi.org/10.1021/acsomega.4c02646
ACS Omega 2024, 9, 34567−34576